SPECTROSCOPIC STUDIES OF OH IN FLAMES

I. THEORETICAL INVESTIGATIONS OF DISTORTIONS PRODUCED BY TEMPERATURE GRADIENTS, SELF-ABSORPTION, AND CHANGES IN SPECTRAL LINE-SHAPE.

II. EXPERIMENTAL STUDIES ON ACETYLENE-OXYGEN FLAMES BURNING AT ATMOSPHERIC PRESSURE.

Thesis by

B. H. Elliott

Lieutenant Colonel, United States Marine Corps

In Partial Fulfillment of the Requirements

For the Degree of

Aeronautical Engineer

California Institute of Technology

Pasadena, California

1953

ACKNOWLEDGEMENT

The author is indebted to Dr. S. S. Penner for suggesting the studies in combustion spectroscopy and for help with the theoretical studies and with the interpretation of the experimental data. The author also wishes to express his sincere gratitude to Dr. P. J. Dyne and to Mr. D. Weber of Jet Propulsion Laboratory for active assistance with the experimental program, to Dr. H. S. Tsien for helpful comments, and to Dr. R. M. Badger for advice concerning the experimental arrangement in two-path experiments. Thanks are due to Mr. N. Schroeder who performed most of the calculations.

The author wishes to express his appreciation to Professor W. R. Varney for the use of the spectroscopic equipment and facilities and to Lt. H. R. Poorman, U.S.N., for the use of the burner devices.

The author also wishes to express his appreciation to Miss Ruth Winkel for her assistance in the typing of the thesis.

ABSTRACT

A theoretical investigation has been made to determine quantitatively the effects of temperature gradients, self-absorption, and spectral line-shape on the apparent rotational temperatures of OH.

Emission experiments have been performed on the inner cone and on the outer cone of an oxygen-acetylene flame to determine the rotational temperature of the upper energy state of OH.

TABLE OF CONTENTS

LIST OF FIGURES

LIST OF SYMBOLS

Symbol	Definition
$^2\Sigma$	appropriate spectroscopic notation for the ground electronic state of OH
$^2\pi$	appropriate spectroscopic notation for the first excited electronic state of OH
E	energy level
K	rotational quantum number
^3P, ^2S	designations of an atomic orbital
P_{max}	maximum absorption coefficient
X	optical density of the emitters = product of partial pressure of emitter and of optical pathlength
a	line -shape parameter
ϵ'	self-absorption parameter
$I_{max}(K)$	peak intensity of radiation emitted from the K'th line
b_N, b_C, b_D	natural, collision, and doppler half-widths
$S_{\ell u}(K)$	integral of the spectral absorption coefficient for the K'th line
c	velocity of light
N_u	number of molecules per unit volume per unit pressure in the upper energy state
N	total number of molecules per unit volume per unit pressure
$\nu_{\ell u}$	frequency of the emitted or absorbed radiation at the center of a line, which is obtained from the Bohr frequency relation
$q_{\ell u}$	matrix element corresponding to transitions between two given energy states

Symbol	Definition
$\rho^{o}(\nu_{\ell u})$	volume density of blackbody radiation at the frequency $\nu_{\ell u}$ as given by the Planck distribution law
$g_u(K)$	statistical weight of the upper energy state involved in the given transition from level K
Q	complete partition function
T_s	temperature of light source
h	Planck's constant
k	Boltzmann constant
Å	Angstrom unit = 10^{-8} cm.
$P(\omega_{\ell u})$	spectral absorption coefficient at the line center

I. THEORETICAL INVESTIGATIONS OF DISTORTIONS PRODUCED BY TEMPERATURE GRADIENTS, SELF-ABSORPTION, AND CHANGES IN SPECTRAL LINE-SHAPE

A. Introduction

A number of experimental studies have been reported on the population temperatures of the $^2\Sigma \rightarrow {}^2\Pi$ transitions of OH in flames at low pressures[1, 2] and at atmospheric pressures.[1, 3, 4] Using conventional techniques[1, 2, 4] to treat the experimental data, the plots that are used for the determination of rotational temperatures are sometimes found to exhibit discontinuities or curvatures both in the region of small and of large values of the rotational energy E(K) of the initial (upper) state. The discontinuities observed for small values of K have been attributed to the formation of OH in the excited electronic state by different chemical reactions leading to a bimodal distribution of population densities,[1, 4] to the falsification of experimental data by absorption of emitted radiation by cooler gas layers through which the flame is viewed,[4] and to self absorption.[5] Some of the observed curvatures for large values of K have been interpreted to indicate predissociation according to the process

$$OH(^2\Sigma^+) \rightarrow OH(^2\Sigma^-) \rightarrow O(^3P) + H(^2S).$$

It has been reported previously[6] that the best available intensity estimates[7] on OH indicate that the product of the maximum absorption coefficient P_{max} and of the optical density of the emitters X is not small compared to unity for the more intense spectral lines of OH in

representative low pressure flames.

If $P_{max}X$ is not small then the conventional interpretation does not hold. Even the iso-intensity method fails. Quantitative studies of apparent rotational temperatures of OH in emission and absorption for spectral lines with Doppler contour have been published recently.[8] It is the purpose of the present paper to extend these studies and to investigate theoretically the effects of temperature gradients, self-absorption, and spectral line-shape on the apparent rotational temperatures of OH.

In Section B we examine the effect of spectral line-shape and of self-absorption on the use of the iso-intensity method for temperature determination in isothermal systems. Intensities of the K'th spectral line relative to the first spectral line are plotted vs. the rotational quantum number K in Figs. 1 to 3 for the P_1-branch, $^2\Sigma \rightarrow {}^2\Pi$ transitions of OH, (0, 0) band. The following parameters were used in these calculations: a line-shape parameter $\underline{a}$ which depends upon pressure and a self-absorption parameter ε' which depends upon the amount of OH present. Table I indicates a large effect of ε' for small $\underline{a}$, but results are quite insensitive to ε' for large $\underline{a}$. The conclusion is reached that self-absorption errors become more important as the pressure is decreased. Because of the ambiguity of matching lines of equal intensity for small values of $\underline{a}$ and large values of ε', the iso-intensity method cannot

be used, even for isothermal systems, at low pressures unless independent proof is provided that $\varepsilon' \ll 0.3$.

In Section C a two-path experiment is described for two adjacent isothermal regions and for spectral lines with Doppler contour. Equations are developed for calculating relative peak intensities for two-path and for single-path experiments (I/I'). The results are summarized in Figs. 5 to 8. A study of Figs. 5 to 8 clearly shows that the ratio I/I' is a very sensitive function of the concentrations of OH in the two isothermal regions. Thus a two-path experiment measuring peak intensities is a relatively sensitive device for studying self-absorption and temperature distortion quantitatively.

In Section D an absorption experiment is described for two adjacent isothermal regions for spectral lines with Doppler contour. It is shown that the results obtained in Section C may be reinterpreted to yield the absorptivity for discrete line sources by adjacent isothermal regions. Unlike peak intensity determinations in two-path experiments, the discrete line source experiment may be feasible with ordinary spectroscopic apparatus.

In Section E two-path experiments for two adjacent isothermal regions are considered for spectral lines with combined Doppler and collision broadening.

In Section F absorption experiments are discussed for discrete

line sources and two adjacent isothermal regions for spectral lines with combined Doppler and collision broadening.

The calculations emphasize the fact that definitive conclusions regarding interpretation of flame spectra are not easy to obtain by use of conventional low-resolution spectroscopic studies of flames. Multiple path experiments or absorption studies with discrete line sources appear promising provided they are restricted to conditions under which the spectral line-shape is known. Alternately, the use of interferometric studies may be indicated.

B. Effect of Line-Shape and of Self-Absorption on the Use of the Iso-intensity Method[3] for Isothermal Systems

According to the iso-intensity method the temperature of a radiator is obtained from a comparison of two spectral lines which are of equal intensity. Let A(K) be the total intensity of the line identified by the index K. Then, for spectral lines with Doppler contour,[8]

$$A(K)/A(K') = \left[I_{max}(K)/I_{max}(K')\right]\left[\nu_{lu}(K)/\nu_{lu}(K')\right] \times \left[\xi(K')/\xi(K)\right] \quad (1)$$

where $I_{max}(K)$ is the peak intensity emitted from the K'th line, $\nu_{lu}(K)$ is the frequency at the line center of the K'th line, and $\xi(K)$ is a known function of the value of $P_{max}X$ for the K'th line and is plotted in Ref. 8. Here P_{max} is the maximum spectral absorption

coefficient and X is the optical density. The line-shape for combined Doppler-and collision-broadening is described by the parameter

$$a = (b_N + b_C)\,(\ell n\ 2)^{1/2} / b_D \qquad (2)$$

where b_N, b_C, and b_D denote, respectively, the natural, the collision, and Doppler half-widths. In general $b_N << b_C$ and $a \simeq 0$ for pure Doppler-broadening.

In order to emphasize that Eq. (1) applies to spectral lines with Doppler contour we shall write it as

$$A(a = 0,\ K)/A(a = 0,\ K') = \left[I_{max}(a = 0,\ K)/I_{max}(a = 0,\ K') \right]$$

$$\times \left[\nu_{\ell u}(K)/\nu_{\ell u}(K') \right] \left[\xi(K')/\xi(K) \right] . \qquad (1a)$$

The effect of line-shape, under isothermal conditions, on the use of the iso-intensity method may be determined by evaluating the ratio $A(a, K)/A(a, K')$. This result can be obtained most conveniently by using Eq. (1a) in conjunction with the "curves of growth".[9]

The ordinate of the curve of growth is proportional to $A(a, K)$ for $P_{max}X(K)$. Thus the ratio $A(a, K)/A(a = 0, K)$ can be obtained simply by reading the ordinate corresponding to the known value of $P_{max}X(K)$. Finally, the quantity $A(a,K)/A(a,K')$ is obtained by writing

$$A(a,K)/A(A,K') = \left\{\left[A(a,K)/A(a=0,\ K)\right] \Big/ \left[A(a,K')/A(a=0,\ K')\right]\right\} \times \left[A(a=0,\ K)/A(a=0,\ K')\right]. \qquad (3)$$

The results for $K' = 1$ of representative calculations at $3000^{\circ}K$, using Eqs. (1a) and (3) together with the "curves of growth" [for the P_1-branch of the $^2\Sigma \rightarrow {}^2\pi$ transitions of OH, (0, 0)-band], are plotted in Figs. 1 to 3 for $a = 0.005$, $a = 0.05$, and $a = 2$, respectively. The self-absorption parameter ε' again refers to the value of $1 - \exp(-P_{max}X)$ for the first line of the P_1-branch and assumes the values 0.3, 0.7, and 0.95.

In order to illustrate the combined effects of line-shape and self-absorption on lines of equal intensity, from which conclusions might be drawn concerning the "temperature", the results listed in Table I may be consulted. In Table I the lines of intensity closest to the intensity for $K = 3$ and $K = 6$ have been tabulated for different values of ε' and of $\underline{a}$. Reference to the data shown in Table I indicates a large effect of ε' for small $\underline{a}$, but the results are quite insensitive to ε' for large $\underline{a}$. Hence the conclusion is reached that self-absorption errors become more important as the pressure is reduced, i.e., as $\underline{a}$ is decreased. A more quantitative conclusion is justified only if absolute values are known for $\underline{a}$ in flames, which is not the case at the present time.

Because of the ambiguity in matching lines of equal intensity for small values of a and large values of ε' the iso-intensity method cannot be used, even for isothermal systems, at low pressures unless independent proof is provided that $\varepsilon' << 0.3$.

If ε' is sufficiently small then it can be shown that

$$A(a,K)/A(a,K') = S_{\ell u}(K)/S_{\ell u}(K') \qquad (4)$$

Table I. Effect of ε' and a on Lines of Equal Total Intensity.

	K value of line with intensity closest to K = 3 for		
	$\varepsilon' = 0.3$	$\varepsilon' = 0.7$	$\varepsilon' = 0.95$
a = 0.005	13	14	16
a = 0.05	13	14	16
a = 2	13	13	14
	K value of line with intensity closest to K = 6 for		
	$\varepsilon' = 0.3$	$\varepsilon' = 0.7$	$\varepsilon' = 0.95$
a = 0.005	10	11	14
a = 0.05	10	11	13
a = 2	10	10	10

where $S_{\ell u}(K)$ is the integral of the spectral absorption coefficient for the K'th line. Here $S_{\ell u}(K)$ is given by the expression[6]

$$S_{\ell u}(K) = (64\pi^4/3c^3)\, N_u(K) \left[\nu_{\ell u}(K)\right]^4 \left[q_{\ell u}(K)\right]^2 / c\rho^{o}\left[\nu_{\ell u}(K)\right] \quad (5)$$

where c = velocity of light; N_u = number of molecules per unit volume per unit pressure in the upper energy state; $\nu_{\ell u}$ = frequency of the emitted or absorbed radiation at the center of the line, which is obtained from the Bohr frequency relation; $q_{\ell u}$ = matrix element corresponding to transitions between the two given energy states; and $\rho^{o}(\nu_{\ell u})$ = volume density of blackbody radiation at the frequency $\nu_{\ell u}$ as given by the Planck distribution law. The quantity $N_u(K)$ may be replaced by $N_u(K) = Ng_u(K) \times \left[\exp(-E_u(K)/kTu)\right]/Q$ where N = total number of molecules per unit volume per unit pressure, $g_u(K)$ = statistical weight of the upper energy state involved in the given transition, Q = complete partition function, and the expression for $S_{\ell u}(K)$ may be rewritten as

$$S_{\ell u}(K) = (64\pi^4/3c^3)\, Ng_u(K) \left[\nu_{\ell u}(K)\right]^4 \left[q_{\ell u}(K)\right]^2 \times \left\{\exp\left[-E_u(K)/kTu\right]\right\} Q^{-1} c^{-1} \left\{\rho^{o}\left[\nu_{\ell u}(K)\right]\right\}^{-1}. \quad (5a)$$

Hence, for lines of equal intensity,

$$S_{\ell u}(K)/S_{\ell u}(K') = \left\{\left[\nu_{\ell u}(K)\right]^4 g_u(K)\left[q_{\ell u}(K)\right]^2\right.$$
$$\times\left\{\left[\nu_{\ell u}(K')\right]^4 g_u(K')\left[q_{\ell u}(K')\right]^2\right\}^{-1}$$
$$\times\left\{\rho^\circ\left[\nu_{\ell u}(K')\right]\right\}\left\{\rho^\circ\left[\nu_{\ell u}(K)\right]\right\}^{-1}$$
$$\times \exp\left\{-\left[E_u(K) - E_u(K')\right]/kT_u\right\} \equiv 1 \qquad (6)$$

But

$$\left\{\rho^\circ\left[\nu_{\ell u}(K')\right]\right\}\left\{\rho^\circ\left[\nu_{\ell u}(K)\right]\right\}^{-1} = \left[\nu_{\ell u}(K')\right]^3\left[\nu_{\ell u}(K)\right]^{-3}$$
$$\times\left\{\exp\left[h\,\nu_{\ell u}(K)/\,kT_u\right] - 1\right\}$$
$$\times\left\{\exp\left[h\,\nu_{\ell u}(K')/kT_u\right] - 1\right\}^{-1}$$
$$\cong \left[\nu_{\ell u}(K')\right]^3\left[\nu_{\ell u}(K)\right]^{-3}$$
$$\times \exp\left\{(h/kT_u)\left[\nu_{\ell u}(K) - \nu_{\ell u}(K')\right]\right\}.$$

Substituting this relation in Eq. (6) we obtain

$$1 = \left[\nu_{\ell u}(K)/\,\nu_{\ell u}(K')\right]\left\{g_u(K)\left[q_{\ell u}(K)\right]^2/\,g_u(K')\left[q_{\ell u}(K')\right]^2\right.$$
$$\times \exp\left\{-\left[E_u(K) - E_u(K')\right]/kT_u\right\}$$
$$\times \exp\left\{(h/kT_u)\left[\nu_{\ell u}(K) - \nu_{\ell u}(K')\right]\right\} \qquad (6a)$$

In this last expression every quantity is known for a given pair of lines, except the temperature T_u. Hence Eq. (6a) can be used to obtain T_u as

$$T_u = - \frac{\left[E_u(K) - E_u(K')\right] + h\left[\nu_{\ell u}(K) - \nu_{\ell u}(K')\right]}{k\ell n\left\{\frac{\nu_{\ell u}(K')\, g_u(K')\left[q_{\ell u}(K')\right]^2}{\nu_{\ell u}(K)\, g_u(K)\left[q_{\ell u}(K)\right]^2}\right\}} \qquad (6b)$$

This principle is used in conventional iso-intensity methods for measuring temperatures although the approximation $\nu_{\ell u}(K) \cong \nu_{\ell u}(K')$ is usually added.

It is clear from the preceding discussion that the practical use of Eq. (6b) depends on the identity of $A(a, K)/A(a, K')$ with $S_{\ell u}(K)/S_{\ell u}(K')$. The limitations concerning this relation have been discussed in connection with Figs. 1 to 3 and Table I.

C. Two-Path Experiments for Non-Isothermal Regions (Spectral Lines with Doppler Contour, Peak Intensities).

Calculations which are made in this section correspond to the assumed experimental arrangement illustrated in Fig. 4. The OH concentration is treated as a variable parameter both in the hot region $\left\{\varepsilon = \left[1 - \exp\left(-P_{max}X\right)\right]\right\}$ and in the cool region $\left\{\varepsilon' = \left[1 - \exp\left(-P_{max}'X'\right)\right]\right\}$. It is physically reasonable to assume $\varepsilon' \leq \varepsilon$.

Calculations have been carried out for peak intensities and for spectral lines with Doppler contour. Peak intensities, even for low-pressure flames with Doppler-broadened lines, have not been measured. Such measurements might be possible with an interferometer. In particular, it is clear that the results of the present calculations do not apply to observational data obtained with a low-resolution spectrograph.

Referring to Fig. 4 the peak intensity I for the spectral line whose center lies at $\nu_{\ell u}$ may be written as follows:

$$
\begin{aligned}
I = {} & R'(\nu_{\ell u})\left[1 - \exp(-P_{max}{}'X')\right] \\
& + R(\nu_{\ell u})\left[1 - \exp(-P_{max}X)\right]\exp(-P_{max}{}'X') \\
& + R'(\nu_{\ell u})\left[1 - \exp(-P_{max}{}'X')\right]\exp(-P_{max}X)\exp(-P_{max}{}'X') \\
& + r\Big\{R'(\nu_{\ell u})\left[1 - \exp(-P_{max}{}'X')\right]\exp(-2P_{max}{}'X')\exp(-P_{max}X) \\
& + R(\nu_{\ell u})\left[1 - \exp(-P_{max}X)\right]\exp(-3P_{max}{}'X')\exp(-P_{max}X) \\
& + R'(\nu_{\ell u})\left[1 - \exp(-P_{max}{}'X')\right]\exp(-2P_{max}X)\exp(-3P_{max}{}'X')\Big\}
\end{aligned}
\tag{7}
$$

where r is the reflectivity of the mirror and the other symbols have their usual meaning. Equation (7) may be rewritten in the form

$$I = R'(\nu_{\ell u})\left[1 - \exp(-P_{max}{}'X')\right]$$

$$\left\{1 + \exp(-P_{max}X - P_{max}{}'X') + r\exp(-P_{max}X - 2P_{max}{}'X')\right\}$$

$$+ r\exp(-2P_{max}X - 3P_{max}{}'X')$$

$$+ R(\nu_{\ell u})\left[1 - \exp(-P_{max}X)\right]\exp(-P_{max}{}'X')$$

$$\left\{1 + r\exp(-P_{max}X - 2P_{max}{}'X')\right\}. \qquad (7a)$$

Using Planck's blackbody distribution for $R(\nu_{\ell u})$ it follows that

$$R'(\nu_{\ell u})/R(\nu_{\ell u}) = \exp\left\{-(h\,\nu_{\ell u}/k)\left[(1/T') - (1/T)\right]\right\}.$$

Hence Eq. (7a) becomes

$$I/R(\nu_{\ell u}) = \left[1 - \exp(-P_{max}X)\right]\exp(-P_{max}{}'X')$$

$$\left\{1 + r\exp(-P_{max}X - 2P_{max}{}'X')\right\}$$

$$+ \exp\left\{-(h\,\nu_{\ell u}/k)\left[(1/T') - (1/T)\right]\right\}\left[1 - \exp(-P_{max}{}'X')\right]$$

$$\times\left\{1 + \exp(-P_{max}X - P_{max}{}'X') + r\exp(-P_{max}X - 2P_{max}{}'X')\right.$$

$$\left. + r\exp(-2P_{max}X - 3P_{max}{}'X')\right\}. \qquad (7b)$$

For reasonable values of T and T' and for unit reflectivity of the mirror we obtain:

$$I \simeq R(\nu_{\ell u})\, \varepsilon\, (1 - \varepsilon') \left[1 + (1 - \varepsilon)(1 - \varepsilon')^2\right] \tag{8}$$

If I' represents the intensity for the single path, then $I' \simeq R(\nu_{\ell u})\, \varepsilon\, (1 - \varepsilon')$ whence

$$I/I' \simeq 1 + (1 - \varepsilon)(1 - \varepsilon')^2 . \tag{9}$$

The observable ratio I/I' has been calculated as a function of K for various values of ε (K = 1) and ε' (K = 1) for the P_1-branch and $^2\Sigma \rightarrow {}^2\pi$ transitions of OH. Results are plotted in Figs. 5 to 8. Reference to Figs. 5 to 8 shows that the intensity ratio $I(K)/I'(K)$ is a very sensitive function of the self absorption parameters ε and ε'. It is clear that the intensity ratio for two-path experiments would be a much less sensitive function of ε and ε' for measurements of total intensity.

The important result derived from the present calculations is that even for values of ε as small as 0.3 the ratio $I(K)/I(K')$ is appreciably less than two for the stronger lines. In other words, a two-path experiment measuring peak intensities is a relatively sensitive device for studying self-absorption and temperature-distortion quantitatively. As will be shown in the following Section D, this last conclusion applies also to absorption experiments in

which peak intensities are measured.

D. Absorption Experiment for Non-Isothermal Regions (Spectral Lines with Doppler Contour, Peak Intensities).

Because of the experimental difficulties arising from inadequate resolving power in the measurement of peak intensities for two-path experiments, it is of interest to consider the use of absorption experiments using discrete line sources.

Calculations which are made in this section correspond to the assumed experimental arrangement illustrated in Fig. 9. The light source radiates at the center of a given spectral line as a blackbody at the temperature T_s.

Referring to Fig. 9, the transmitted intensity I* for the spectral line whose center lies at $\nu_{\ell u}$ may be written as follows:

$$I^* = R(T_s) \exp(-2P_{max}'X' - P_{max}X)$$
$$+ R(T') \left[1 - \exp(-P_{max}'X')\right]$$
$$+ R(T)\left[1 - \exp(-P_{max}X)\right] \exp(-P_{max}'X')$$
$$+ R(T') \left[1 - \exp(-P_{max}'X')\right] \exp(-P_{max}X - P_{max}'X'). \qquad (10)$$

For $T_s >> T$, T' and $\exp(-P_{max}X)$, $\exp(-P_{max}'X') << 1$,

$$I^* = R(T_s) \exp(-2P_{max}'X' - P_{max}X). \qquad (10a)$$

From Eq. (10):

$$I^*/R(T_s) = \exp(-2P_{max}{}'X' - P_{max}X) + R(T')/R(T_s)\left[1 - \exp(-P_{max}{}'X')\right] \times \left[1 + \exp(-P_{max}X - P_{max}{}'X')\right] + R(T)/R(T_s)\left[1 - \exp(-P_{max}X)\right]\exp(-P_{max}{}'X') \quad (10b)$$

or

$$I^*/R(T_s) = \exp(-2P_{max}{}'X' - P_{max}X) + \exp\left\{-(h\nu_{\ell u}/k)\left[(1/T') - (1/T_s)\right]\right\}\left[1 - \exp(-P_{max}{}'X')\right] \times \left[1 - \exp(-P_{max}X - P_{max}{}'X')\right] + \exp\left\{-(h\nu_{\ell u}/k)\left[(1/T') - (1/T_s)\right]\right\} \times \left[1 - \exp(-P_{max}X)\right]\exp(-P_{max}{}'X'). \quad (10c)$$

In general we may neglect the radiation from the region at temperature T' and use the relation

$$I^*/R(T_s) = \exp(-2P_{max}{}'X' - P_{max}X) + \exp\left\{-(h\nu_{\ell u}/k)\left[(1/T) - (1/T_s)\right]\right\} \times \left[1 - \exp(-P_{max}X)\right]\exp(-P_{max}{}'X') = (1 - \varepsilon')^2(1 - \varepsilon) + \varepsilon(1 - \varepsilon')\exp\left\{-(h\nu_{\ell u}/k)\left[(1/T) - (1/T_s)\right]\right\}. \quad (10d)$$

If $T_s >> T$, as should be the case for a good absorption experiment, then

$$\exp\left\{-(h\nu_{\ell u}/k)\left[(1/T - (1/T_s)\right]\right\} \simeq \exp(-h\nu_{\ell u}/kT).$$

But $h\nu/k = hc\omega/k = 1.432$ and $\exp(-h\nu_{\ell u}/kT)$

$$\simeq \exp(1.432 \times 30,000/3000) \simeq \exp(-14).$$

Hence for $T_s >> T$ Eq. (10d) may be written as

$$I^*/R(T_s) \simeq (1 - \varepsilon')^2 (1 - \varepsilon). \qquad (11)$$

Comparison of Eqs. (9) and (11) shows that the transmitted intensity divided by the incident intensity from a discrete line source is nearly equal to $I/I' - 1$ where I/I' is the ratio of the intensity of the flame for a double-path experiment to the intensity of the flame for a single-path experiment. Figures (5) to (8) may then be reinterpreted in such a way that $I/I' - 1$ represents the transmissivity of the flame for discrete radiation.

Since I/I' or $I/I' - 1$, for measurements of peak intensities, are very sensitive functions of the self absorption parameters ε and ε', it follows that $I^*/R(T_s)$ is also a sensitive function of ε and ε'. Unlike peak intensity determinations in two-path experiments, the discrete line source experiment may be feasible with ordinary spectroscopic apparatus by using as source OH in a discharge tube or else an excited metal line which coincides

exactly with a line of OH.* In this connection it is of interest to note that the 3063.97 Å line of tungsten coincides with the 10' line of the (0, 0) band, $^2\Sigma \rightarrow {}^2\pi$ transitions of OH.

E. Two-Path Experiments for Non-Isothermal Regions (Spectral Lines with Combined Doppler and Collision Broadening, Peak Intensities).

The calculations summarized in this section again correspond to the experimental arrangement illustrated in Fig. 4 of Section B. The parameter P_{max} must now be replaced by $P(\omega_{\ell u})$ where $P(\omega_{\ell u})$, the spectral absorption coefficient at the line center, is to be evaluated for combined Doppler- and collision- broadening. The quantity $P(\omega_{\ell u})$ is related to P_{max} and $\underline{a}$ through the expression[9]

$$P(\omega_{\ell u}) = P_{max}\left[\exp(a^2)\right]\left[\operatorname{erfc}(a)\right] \tag{12}$$

where

$$\operatorname{erfc}(a) = \left[2/\pi^{(1/2)}\right]\int_a^{\infty}\left[\exp(-x^2)\right]dx.$$

Equation (9) may be rewritten as

$$I/I' \simeq 1 + (1 - \varepsilon_{D-C})(1 - \varepsilon'_{D-C})^2 \tag{9a}$$

---

* Absorption experiments using discrete lines as source have been considered at various times by most of the active workers in combustion spectroscopy.

where

$$\varepsilon_{D\text{-}C} = 1 - \exp\left[-(P_{max}X)\ \mathrm{erfc}\ (a)\ \exp\ (a^2)\right], \qquad (13)$$

$$\varepsilon'_{D\text{-}C} = 1 - \exp\left[-(P_{max}'X')\ \mathrm{erfc}\ (a')\ \exp\ (a'^2)\right], \qquad (13a)$$

and a' represents the line-shape parameter for the gases at the temperature T'.

The ratio I/I' has been calculated for $a' = a$ ranging from 0 to 10, $\varepsilon\ (K = 1) = 0.7$, $\varepsilon'(K = 1) = 0.1$ and 0.5, for the P_1-branch, (0, 0)-band and $^2\Sigma \rightarrow {}^2\pi$ transitions of OH. Results are plotted in Figs. 10 and 11. Reference to Figs. 10 and 11 shows that two-path experiments will yield results which are sensitive functions of the line-shape parameter a, with distortion of experimental data by self-absorption diminishing as the numerical value of a is increased, under otherwise comparable experimental conditions.

F. Peak Absorption Experiments for Non-Isothermal Regions (Spectral Lines with Combined Doppler and Collision Broadening).

Calculations in this section correspond to the experimental arrangement illustrated in Fig. 9 of Section C with P_{max} replaced by $P(\omega_{\ell u})$. Here $P(\omega_{\ell u})$ again depends on P_{max} and a as shown in Eq. (12).

Equation (11) now becomes

$$I^*/R(T_s) \simeq (1 - \varepsilon_{D-C})(1 - \varepsilon'_{D-C})^2 \qquad (11a)$$

where ε_{D-C} and ε'_{D-C} have been defined in Eqs. (13) and (13a). Comparison of Eqs. (9a) and (11a) shows that $I^*/RT_S = I/I' - 1$ is obtained simply by reinterpreting the ordinates of Figs. 10 and 11. Hence the same conclusions apply to absorption experiments with discrete sources as to measurements of peak intensities for two-path experiments.

II. EXPERIMENTAL STUDIES ON ACETYLENE-OXYGEN FLAMES BURNING AT ATMOSPHERIC PRESSURE

A. Description of Apparatus

1. Spectrograph*

The arrangement for the experiment is illustrated in the photograph of Fig. 12. Radiation from the flame F, is focused on the slit S, of the 1.5 meter grating spectrograph SG, by a quartz lens L of 3 inch focal length and 1.4 inches in diameter. The grating used in the instrument has a radius of curvature of 1.5 meters, length of line 1 inch and a ruled surface 2 inches in width. There are 24,400 lines per inch, giving a linear dispersion of approximately 7.0 Å per mm in the first order. The radiation is reflected from the grating G, onto a 15 inch strip of 35 mm film in the camera C. The camera is provided with a ratchet allowing ten settings on each film. It was found that not more than three settings, together with a setting for the comparison spectrum, could be used without producing overlapping of the spectrum lines.

2. Densitometer**

The relative intensities of the spectrum lines were obtained

---

* A standard 1.5 meter Applied Research Laboratories Dietert grating spectrograph was used.

** The densitometer used is Model No. 5400 and was manufactured by the Applied Research Laboratories in Glendale, California.

by means of a recording instrument and also by using a visual Film Comparator Densitometer.

3. Flame

An oxygen-acetylene welder's torch tip was used as light source since it is known that in the oxygen-acetylene flame the OH bands appear with very high intensity. Diameters of burners used were .0465 inches and .07 inches. Tank gases* were employed and controlled at approximately 5 lb/in^2 gauge pressure by regulators on the tanks. Needle valves controlled the flow of gas into a mixing chamber on the back of a board, B. The mixing chamber, a cast iron pipe, was approximately 3 inches in diameter and 18 inches long, and filled with glass beads. Calibrated flow meters, CF, of the floating ball type were used for flow measurements Cf. Fig. 12 , readings were accurate to about 5 per cent.

4. Film Calibration

Fully exposed film in the 3100 Å region could be obtained, using Eastman Spectrum Analysis Film No. 1, in about 3 minutes when the spectrograph was focused on the inner cone; exposures of about 15 minutes were required for measurements on the outer cones. Lean mixture ratios, corresponding to approximately one half of stoichiometric, were used. A rotating four step sector, SS, was

---

* The gases were purchased from Linde Air Products Co. Gas purities were specified by the manufacturer as follows: oxygen 99.7 per cent and acetylene, 98 per cent.

provided on the spectrograph by means of which film calibration could be obtained, following standard procedures.[10]

The film was processed with Eastman Developer D-19 and Film Fixer F-5. Four minutes was allowed for developing and 10 minutes for fixing. The film was then washed for 10 minutes in tap water, followed by washing in distilled water.

5. Alignment of Flame

The flame was aligned with respect to the spectrograph by forming a real image of a 6 to 8 volt head lamp bulb, which was placed at the position of the camera. The primary slit of the spectrograph, as well as the secondary aperture, were opened fully, and the image of the lamp, after passing through the spectrograph, was focused over the burner tip in the region of the flame which was to be photographed. The two-path experiment was performed by aligning the spherical mirror, M (focal length of 19 inches), so that the region of the flame to be studied was centered at the radius of curvature of the mirror.

B. Methods for Determining the Rotational Temperature of the Upper Energy State

1. Standard Emission Experiment

In order to determine the rotational temperature of OH from emission spectra in the absence of self-absorption, the following equation is customarily employed[6]

$$\frac{\partial \ln \left[\int_{\Delta \nu_{\ell u}} R_\nu \, d\nu / (\nu_{\ell u})^4 \, g_u \, (q_{\ell u})^2 \right]}{\partial E_u(K)} = - \frac{1}{kT_u} \qquad (14)$$

where $\int_{\Delta \nu_{\ell u}} R\nu \, d\nu$ is proportional to the measured peak intensity of a line obtained with a low-resolution spectrograph; values of $\nu_{\ell u}$, $g_u (q_{\ell u})^2$, and $E_u(K)$ have been defined in Part I and are tabulated in the report of Dieke and Crosswhite.[5] In practice it is convenient to utilize Eq. (14) in the form

$$\frac{2.303 \partial \log \left\{ \left[\int_{\Delta \nu_{\ell u}} R_\nu \, d\nu \right] \left[(g_u q_{\ell u}{}^2)_K / (g_u \, q_{\ell u}{}^2)_{K=1} \right]^{-1} \right\} \left\{ \left[\nu_{\ell u}(K) \right]^4 / \left[\nu_{\ell u}(1) \right]^4 \right\}^{-1}}{\partial E_u}$$

$$= - \frac{1}{kTu} \, . \qquad (15)$$

Equations (14) and (15) apply only to isothermal systems.

2. Two-Path Experiments for Isothermal Systems

In order to determine the rotational temperature of OH from a two-path experiment it is necessary first to estimate a value for the line-shape parameter, a. Once a is known, we may obtain $P_{max}X$ from theoretical curves giving f as a function of $P_{max}X$ for isothermal systems,[11] where f corresponds to the observable

ratio of total intensity for the single-path to the double-path. The temperature may then be obtained from the equation[12]

$$\frac{\partial \ln \left\{ P_{max}(K) X / \left[g_u (q_u)^2 K \right] \right\}}{\partial (E_u - h\nu_{\ell u})} = -1/kT_u. \qquad (16)$$

All errors arising from self-absorption are eliminated by using Eq. (16) which, however, is valid only for isothermal emitters and requires accurate estimates of both $\underline{a}$ and of $P_{max}X$. At the present time the uncertainties in the value of $\underline{a}$ are such that no satisfactory application of Eq. (16) is possible.

C. Experimental Data on Acetylene-Oxygen Flames*

1. Standard Emission Experiment on the Inner Cone

A temperature of 3270°K was obtained from a standard emission experiment on the "inner cone" with an oxygen-acetylene flame in which the fuel to oxygen ratio was one quarter of the stoichiometric ratio. The calculated and experimental data which were used in Eq. (15) are summarized in Table II and are plotted in Fig. 13. Reference to Fig. 13 shows considerable scatter of the experimental data especially for the points corresponding to small

---

* The experimental data refer to the P_1-branch, $^2\Sigma \rightarrow {}^2\pi$ transition, (0, 0)-band of OH.

values of K. It should be noted that the apparent rotational temperature is somewhat higher than the adiabatic flame temperature, in accordance with the experimental findings of other investigators. However, the significance of this result cannot be assessed without auxiliary studies concerning distortion of data by temperature gradients and by self-absorption.

2. Two-Path Experiments on the Outer Cone

As a first attempt to assess the suitability of two-path experiments for spectroscopic studies of flames burning at atmospheric pressure, measurements were performed on the outer cone of an acetylene-oxygen flame (fuel to oxygen ratio equal to one half of the stoichiometric value). Considerable care was exercised in order to align the spherical mirror properly.

The results of a single-path and of a two-path experiment are summarized in Table III. Conventional plots, using Eq. (15), of the experimental data are shown in Figs. 14 and 15. Apparent temperatures of about 4000^{o}K were obtained, although the scatter of the experimental data was considerable.

It is clear that the apparent rotational temperatures are too high since they exceed the adiabatic flame temperature in a region in which thermodynamic equilibrium is known to exist. It is, however, easily shown that the results are not significant and that extensive distortion of experimental data by self-absorption must have occurred.

In Table IV the measured intensity ratio for the two-path experiment to the single-path experiment is shown as a function of K. Reference to Table IV shows that R goes through a pronounced minimum near K = 8, the maximum difference in intensity corresponding to about 40 ^{o}/o. A result of this sort is in accord with the idea that the concentration of OH is too large to justify the use of conventional methods of interpretation of experimental data.

In view of the lack of quantitative information concerning the line-shape parameter $\underline{a}$, it is not possible to use the data shown in Table IV for quantitative estimates of T_u. However, it is clear that for all possible values of $\underline{a}$, the value of $P_{max}X$, for example, for line line K = 2, cannot be small compared to unity. For $\underline{a}$ = 2, the use of available theoretical data[11] leads to results such as $P_{max}(9)X \simeq 18$, $P_{max}(2)X \simeq 6$, etc., which are in rough accord with theoretical predictions based on absolute intensity estimates for representative lines of OH.[6]

Unfortunately time did not permit more extensive quantitative applications of two-path experiments. On the basis of the results obtained in the present investigations it is apparent that the use of multiple-path techniques for quantitative measurements on the inner cones of flames burning at atmospheric pressure presents considerable experimental and theoretical difficulties. However,

the method appears to be relatively easy to apply if one is interested only in determining semi-quantitatively the extent of distortion of data by self-absorption.

Table II. Calculated and Experimental Data for Standard Emission Experiment on Inner Cone.

K	① $\int R_\nu d\nu$	② $\log \int R_\nu d\nu$	③ $\left[\frac{\nu_{eu}(K)}{\nu_{eu}(1)}\right]^{\frac{4}{x}} \frac{(q_u q_{eu}^2)_K}{(q_u q_{eu}^2)_1}$	④ $\log$ ③	⑤ ② − ④	⑥ $E_u(K)$
1			1.0000			32474.62
2	.195	-.70997	1.3425	0.12791	-.83788	542.56
3			1.7338	0.23900		644.22
4			2.1404	0.33050		779.49
5	.271	-.56703	2.5412	.40504	-.97207	948.31
6	.295	-.53018	2.9462	.46926	-.99944	33150.14
7			3.3451	.52441		384.97
8			3.7361	.57242		652.29
9	.369	-.43297	4.1203	.61493	-1.04790	951.80
10			4.4867	.65193		34282.99
11	.330	-.48149	4.8554	.68623	-1.16772	645.53
12			5.2155	.71730		35038.61
13	.265	-.57675	5.5573	.74486	-1.32161	462.01
14	.286	-.54363	5.8997	.77083	-1.31446	914.82
15	.216	-.66555	6.2236	.79404	-1.45959	36396.66
16	.237	-.62525	6.5470	.81604	-1.44129	906.50
17	.185	-.73283	6.8517	.83580	-1.56863	37443.91
18			7.1460	.85406		38007.90
19	.165	-.78252	7.4390	.87152	-1.65404	597.79
20			7.7122	.88718		39212.69
21			7.9747	.90171		851.66
22			8.2255	.91516		40513.79

Table III. Calculated and Experimental Data for Single and Double Path Emission Experiment on Outer Cone.

K	① $\int R_\nu d\nu$	② log ①	③ $\left[\frac{\nu_{eu}(K)}{\nu_{eu}(1)}\right]^2 \times \frac{(q_u q_{eu}^2)_K}{(q_u q_{eu}^2)_1}$	④ log ③	⑤ ② − ④	⑥ $E_u(K)$	K	① $\int R_\nu d\nu$	② log ①	④ log ③	⑤ ② − ④
2	.5	−.30103	1.3425	.12791	−.42894	32542.56	2	.71	−.14874	.12791	−.27665
5	.62	−.20761	2.5412	.40504	−.61265	32948.31	5	.8	−.09691	.40504	−.50195
6	.65	−.18709	2.9462	.46926	−.65635	33150.14	6	.86	−.06550	.46926	−.53476
9	.7	−.1549	4.1203	.61493	−.76983	33951.80	9	.88	−.05552	.61493	−.67045
11	.65	−.18709	4.8554	.68623	−.87332	34645.53	11	1.05	+.02119	.68623	−.66504
13	.53	−.27572	5.5573	.74486	−1.02058	35462.01	13	.86	−.06550	.74486	−.81036
14	.5	−.30103	5.8997	.77083	−1.07186	35914.82	14	.82	−.08619	.77083	−.85702
15	.43	−.36653	6.2236	.79404	−1.16057	36396.66	15	.72	−.14267	.79404	−.93671
16	.435	−.36151	6.5470	.81604	−1.17755	36906.50	16	.76	−.11919	.81604	−.93523
17	.295	−.53018	6.8517	.83580	−1.36598	37443.91	17	.5	−.30103	.83580	−1.13683
19	.185	−.73283	7.4390	.87151	−1.60434	38597.79	19	.31	−.50864	.87151	−1.38015
21	.125	−.90309	7.9747	.90171	−1.8048	39851.66	21	.18	−.74473	.90171	−1.64644

Table IV. Measured Intensity Ratio for Two-Path Experiment to Single-Path Experiment

K	$I_{S.P.}$ Intensity of Single Path	$I_{D.P.}$ Intensity of Double Path	R Ratio of Intensity of Double Path to Intensity of Single Path
2	0.50	0.71	1.42
5	0.62	0.80	1.29
6	0.65	0.86	1.33
9	0.70	0.88	1.26
11	0.65	1.05	1.61
13	0.53	0.86	1.63
14	0.50	0.82	1.64
15	0.43	0.72	1.67
16	0.435	0.76	1.75
17	0.295	0.50	1.70
19	0.185	0.31	1.68
21	0.125	0.18	1.44

REFERENCES

1. A. G. Gaydon and H. G. Wolfhard, Proc. Roy. Soc. (London) A194, 169 (1948); A199, 89 (1949); A201 561 (1950; A201, 570 (1950); A205, 118 (1951); A208, 63 (1951).

2. Penner, Gilbert, and Weber, J. Chem. Phys. 20, 522 (1952).

3. H. P. Broida and K. E. Shuler, J. Chem. Phys. 20, 168 (1952).

4. H. P. Broida, J. Chem. Phys. 19, 1383 (1951).

5. G. H. Dieke and H. M. Crosswhite, "The Ultraviolet Bands of OH", The Johns Hopkins University, Bumblebee Series Report No. 87, (1948).

6. S. S. Penner, J. Chem. Phys. 20, 507 (1952).

7. O. Oldenberg and F. F. Rieke, J. Chem. Phys. 6, 439 (1938); R. J. Dwyer and O. Oldenberg, J. Chem. Phys. 12, 351 (1944).

8. S. S. Penner, J. Chem. Phys. 21, 31 (1953).

9. E. M. F. van der Held, Z. Physik 70, 508 (1931); A. Unsöld, Physik der Sternatmosphären, p. 168, J. W. Edwards, Ann Arbor 1948; for an extension of the curves of growth to larger values of the line-shape parameter a, see S. S. Penner and R. W. Kavanagh, Technical Report No. 6, Contract Nonr-220(03), NR 015 210, Guggenheim Jet Propulsion Center, California Institute of Technology, September 1952, or Journal of the Optical Society of America (*in press*).

10. A.B.C. Harvey, Spectrochemical Procedures, Applied Research Laboratories, Glendale, California p. 47, (1950).

11. S. S. Penner, "Effect of Spectral Line-Shape on Apparent Rotational Temperatures of OH", Technical Report No. 8, Contract Nonr-220(03), NR 015 210, Guggenheim Jet Propulsion Center, California Institute of Technology, Pasadena, California, November, 1952.

12. S. S. Penner, J. Chem. Phys. 20, No. 8, 1341-1342 (1952).

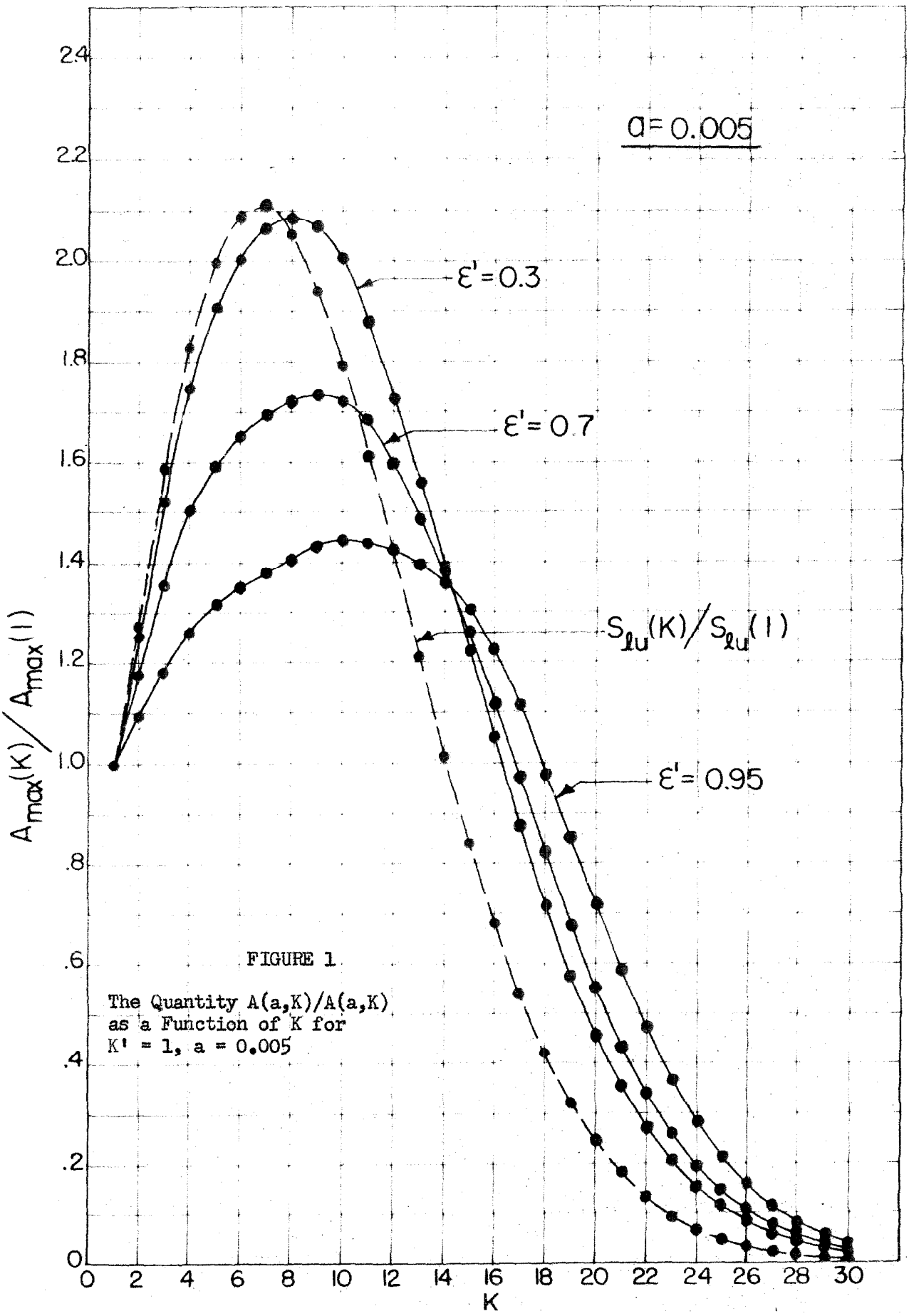

FIGURE 1

The Quantity A(a,K)/A(a,K) as a Function of K for K' = 1, a = 0.005

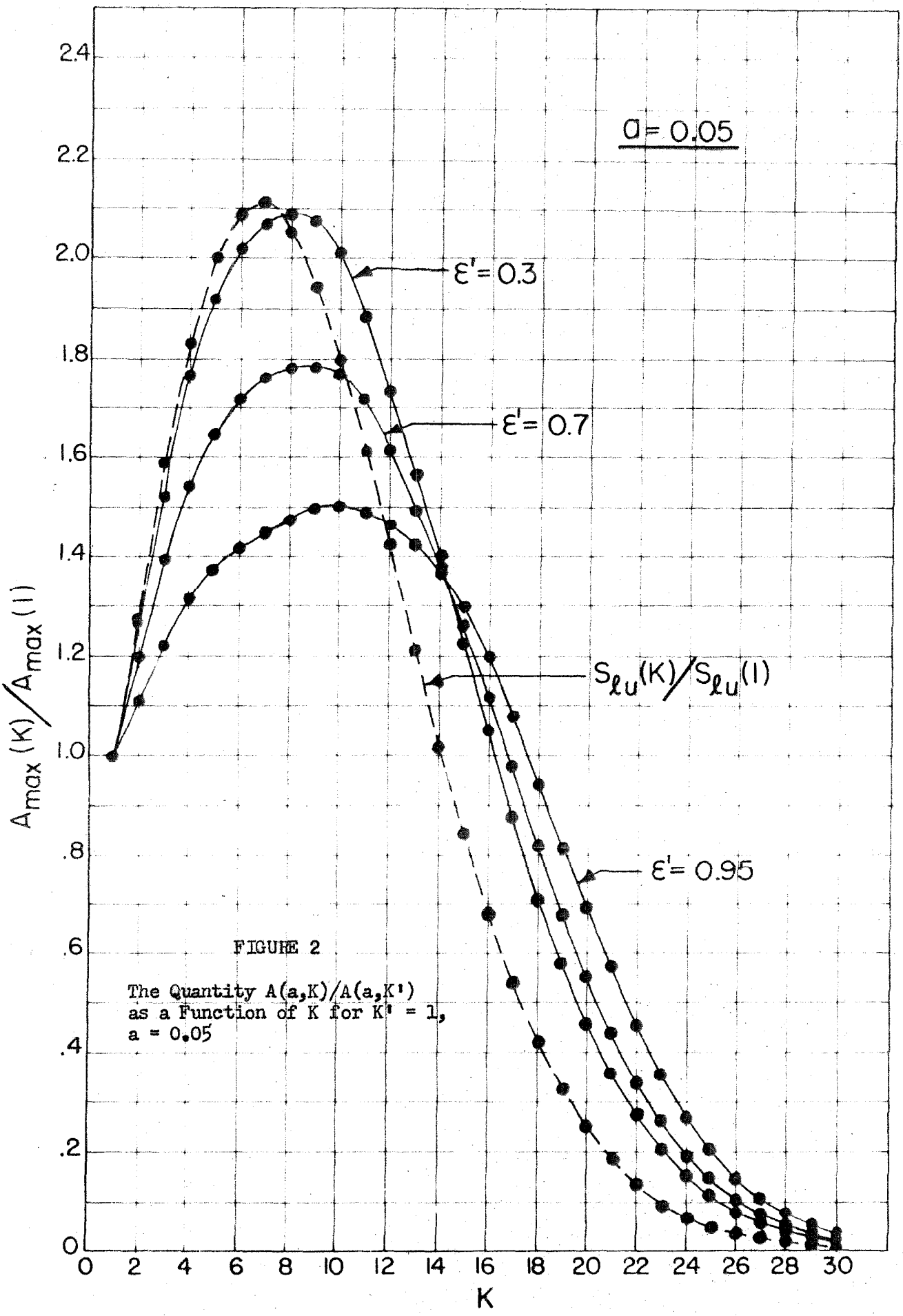

FIGURE 2

The Quantity A(a,K)/A(a,K') as a Function of K for K' = 1, a = 0.05

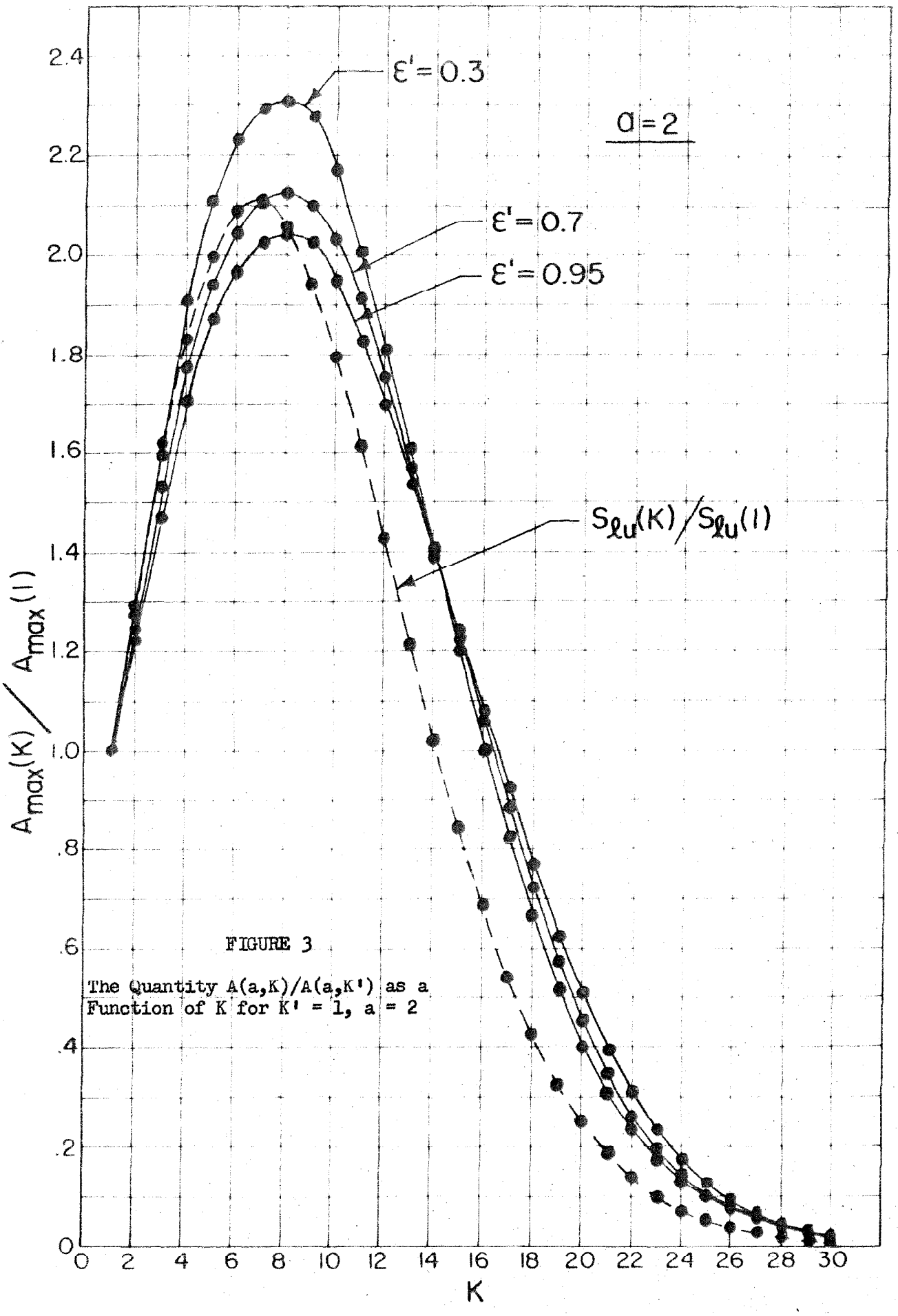

FIGURE 3

The Quantity A(a,K)/A(a,K') as a Function of K for K' = 1, a = 2

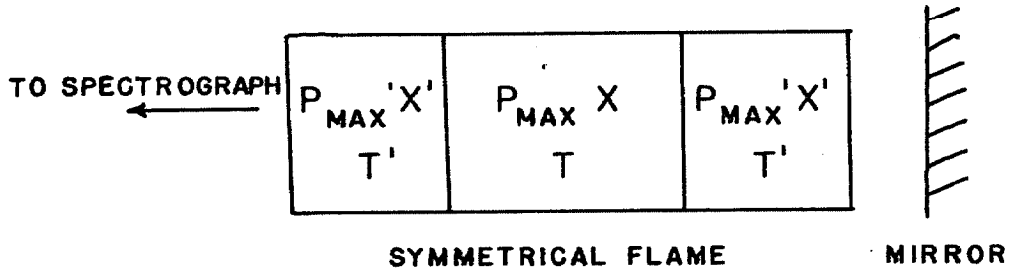

FIG. 4. SCHEMATIC ARRANGEMENT OF TWO-PATH EXPERIMENT FOR A FLAME REPRESENTED BY TWO ISOTHERMAL REGIONS.

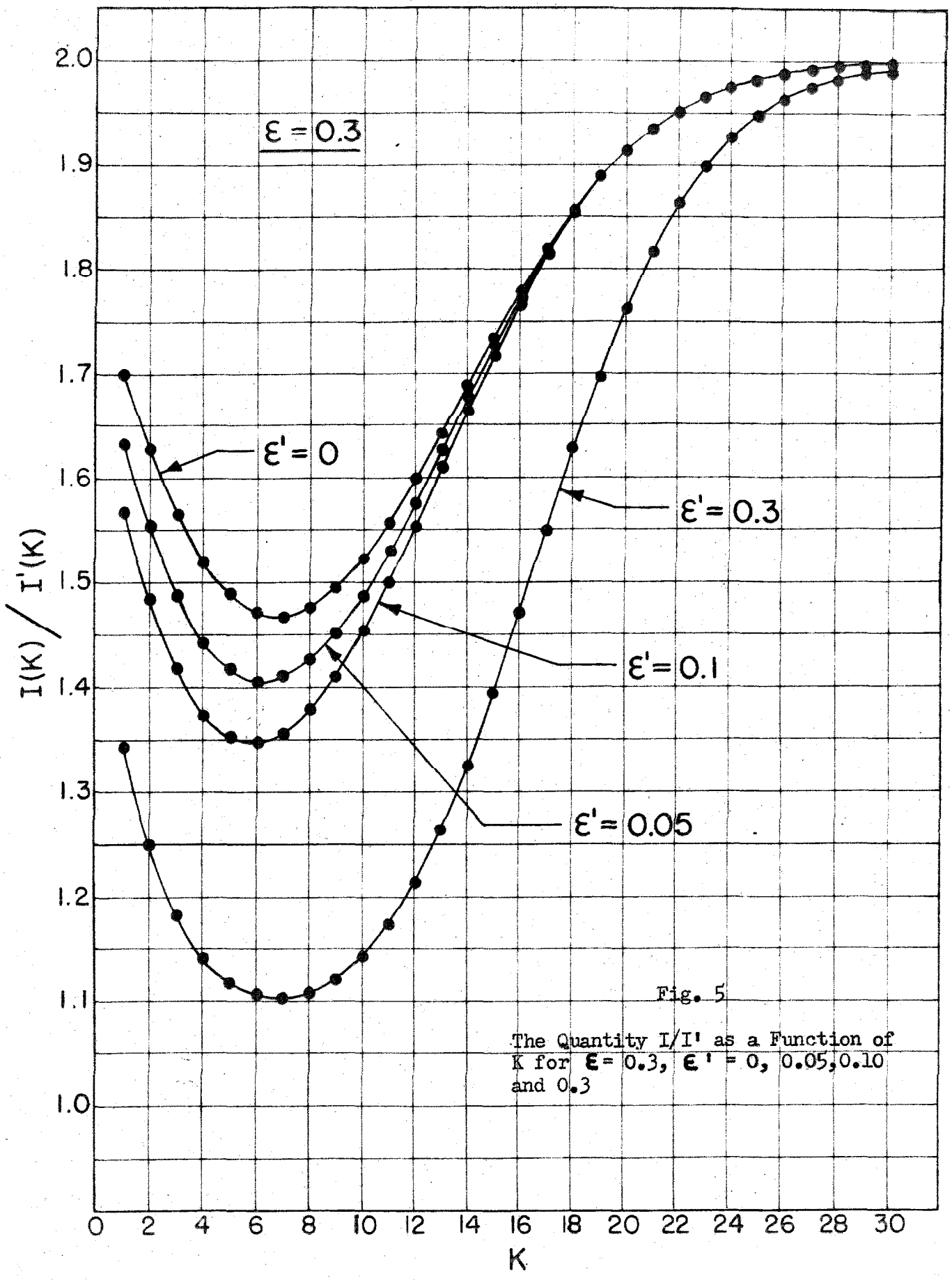

Fig. 5

The Quantity I/I' as a Function of K for $\varepsilon = 0.3$, $\varepsilon' = 0$, 0.05, 0.10 and 0.3

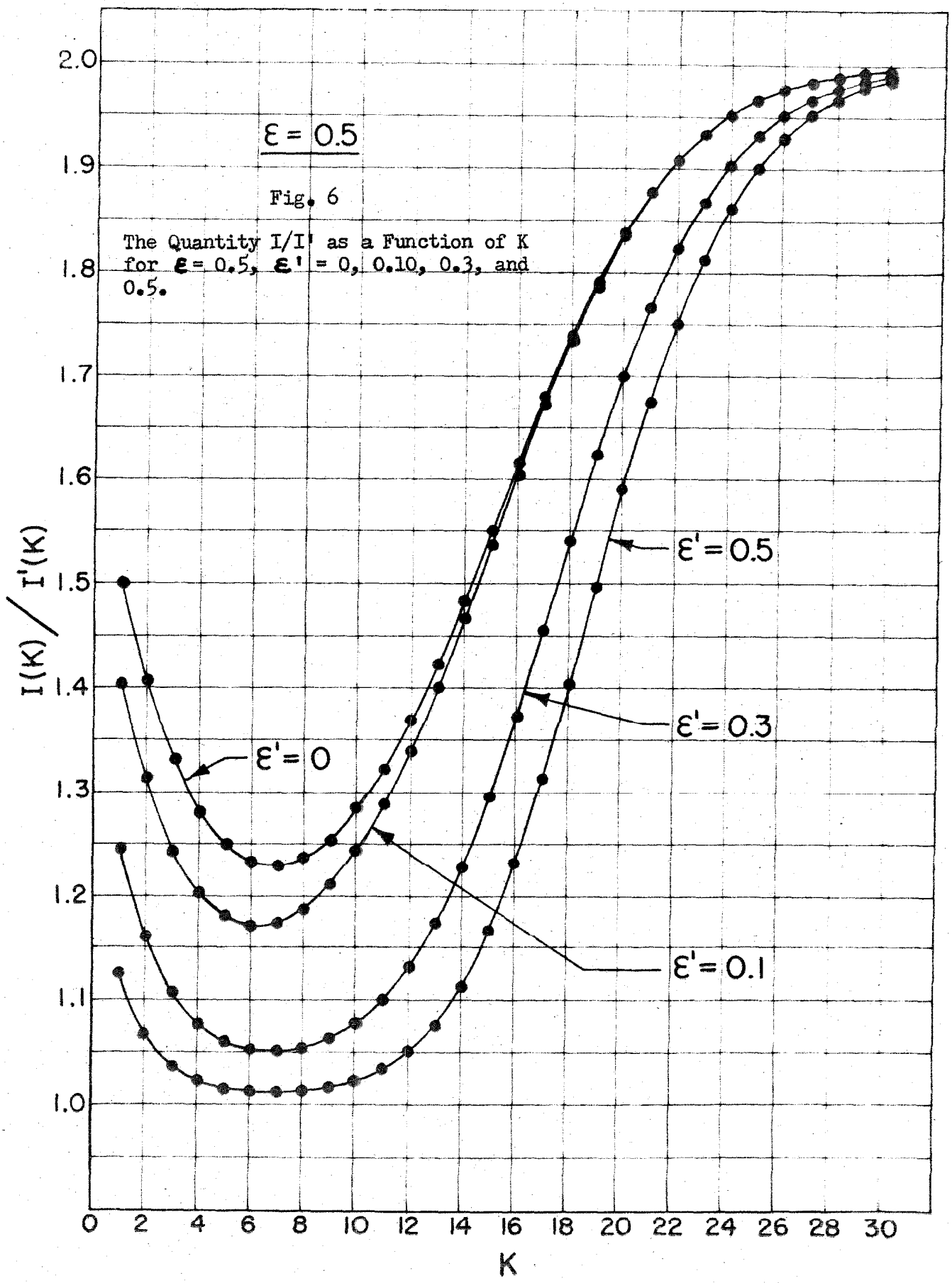

Fig. 6

The Quantity I/I' as a Function of K for $\varepsilon = 0.5$, $\varepsilon' = 0$, 0.10, 0.3, and 0.5.

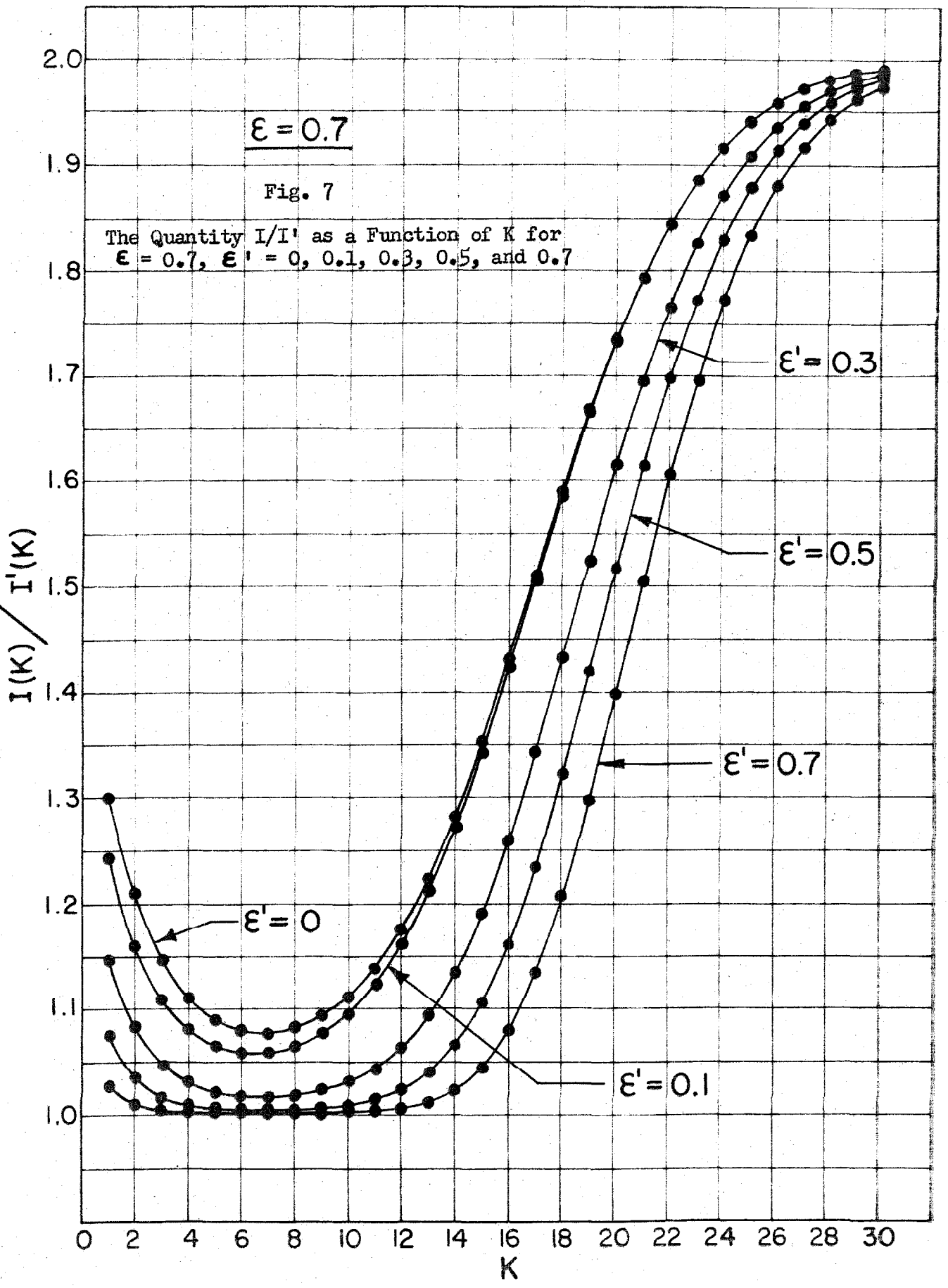

Fig. 7

The Quantity I/I' as a Function of K for $\epsilon = 0.7$, $\epsilon' = 0, 0.1, 0.3, 0.5$, and 0.7

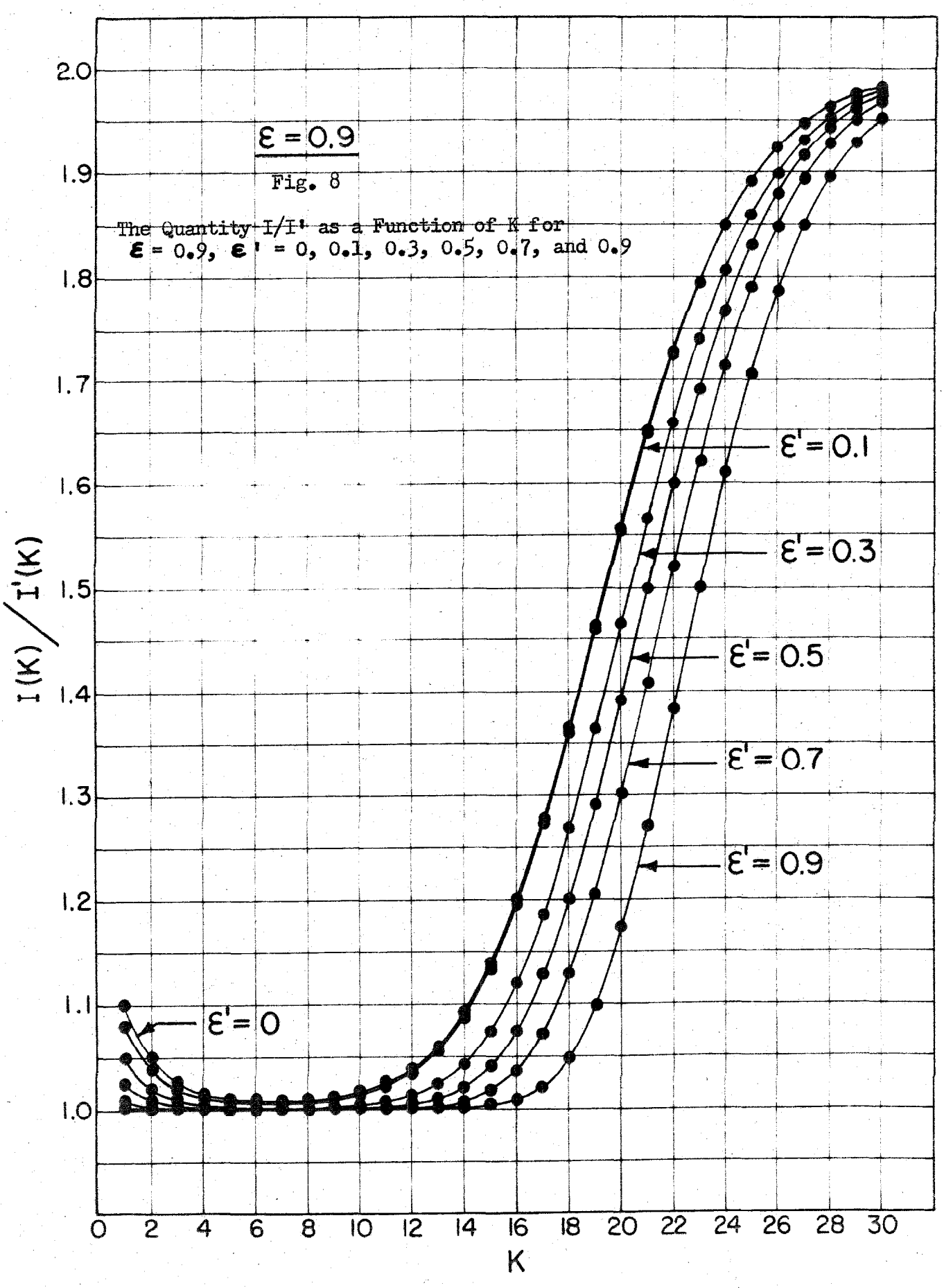

Fig. 8

The Quantity I/I' as a Function of K for
$\varepsilon = 0.9$, $\varepsilon' = 0, 0.1, 0.3, 0.5, 0.7$, and 0.9

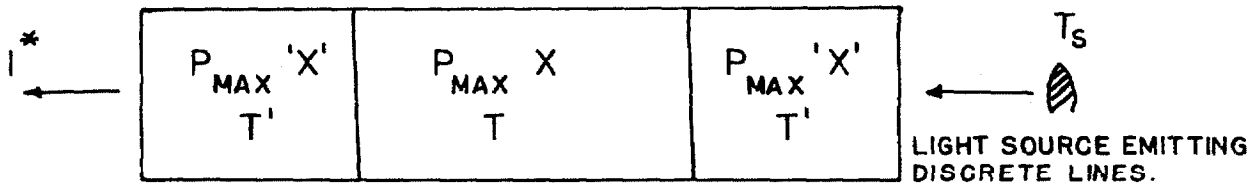

FIG. 9. SCHEMATIC ARRANGEMENT OF ABSORPTION EXPERIMENT FOR A FLAME REPRESENTED BY TWO ISOTHERMAL REGIONS.

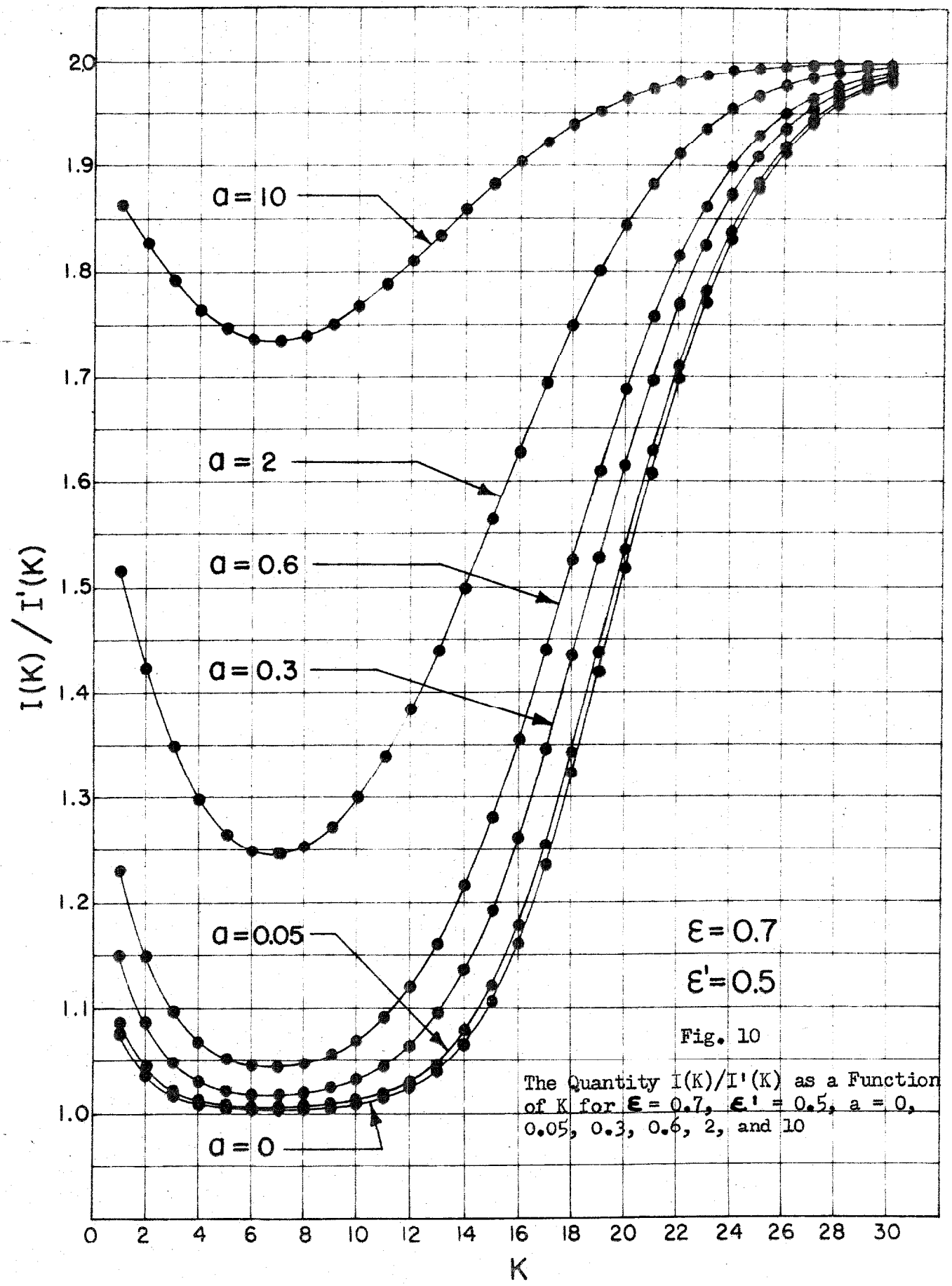

Fig. 10

The Quantity I(K)/I'(K) as a Function of K for $\varepsilon = 0.7$, $\varepsilon' = 0.5$, a = 0, 0.05, 0.3, 0.6, 2, and 10

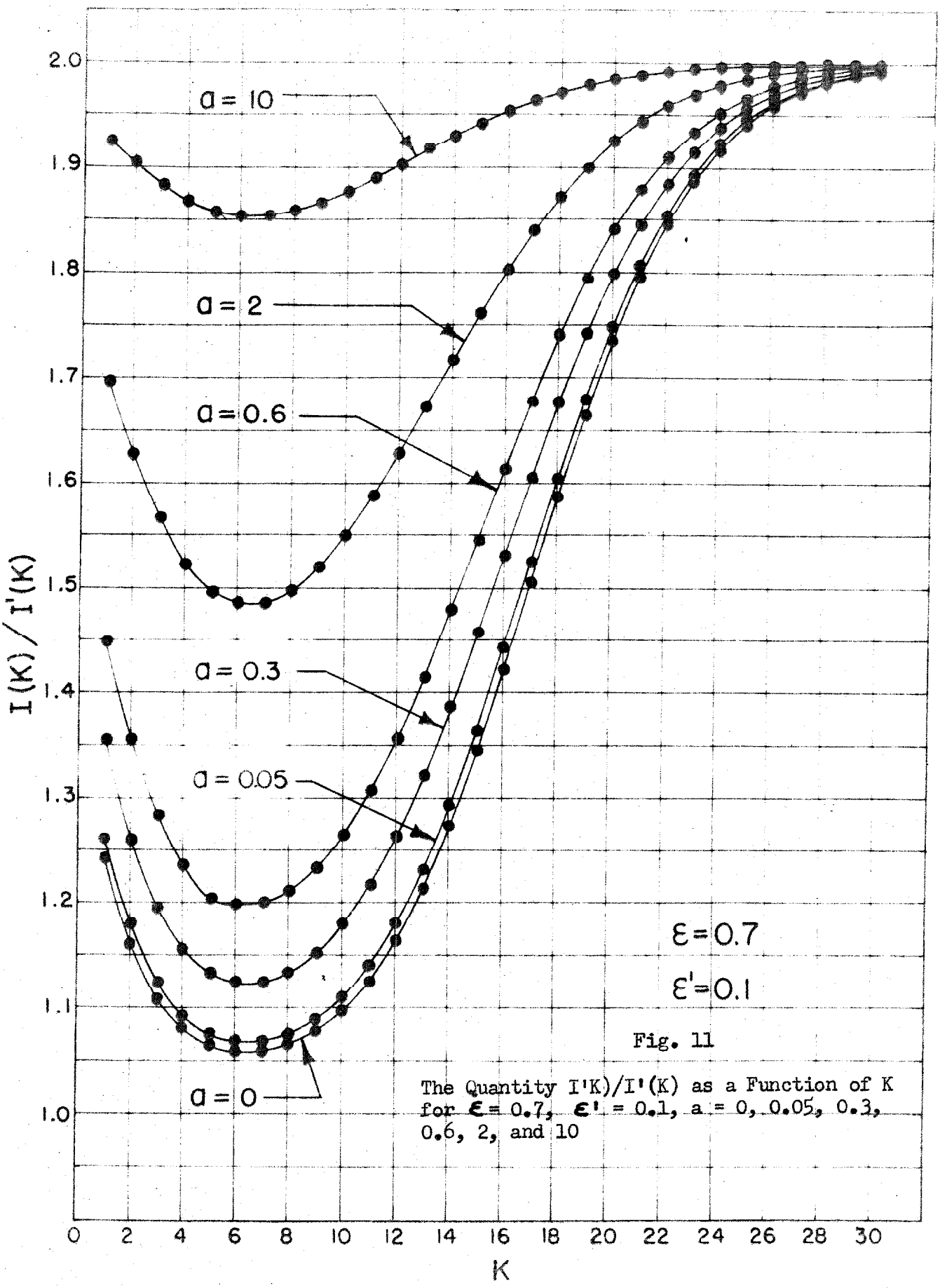

Fig. 11

The Quantity I'K)/I'(K) as a Function of K for $\epsilon = 0.7$, $\epsilon' = 0.1$, a = 0, 0.05, 0.3, 0.6, 2, and 10

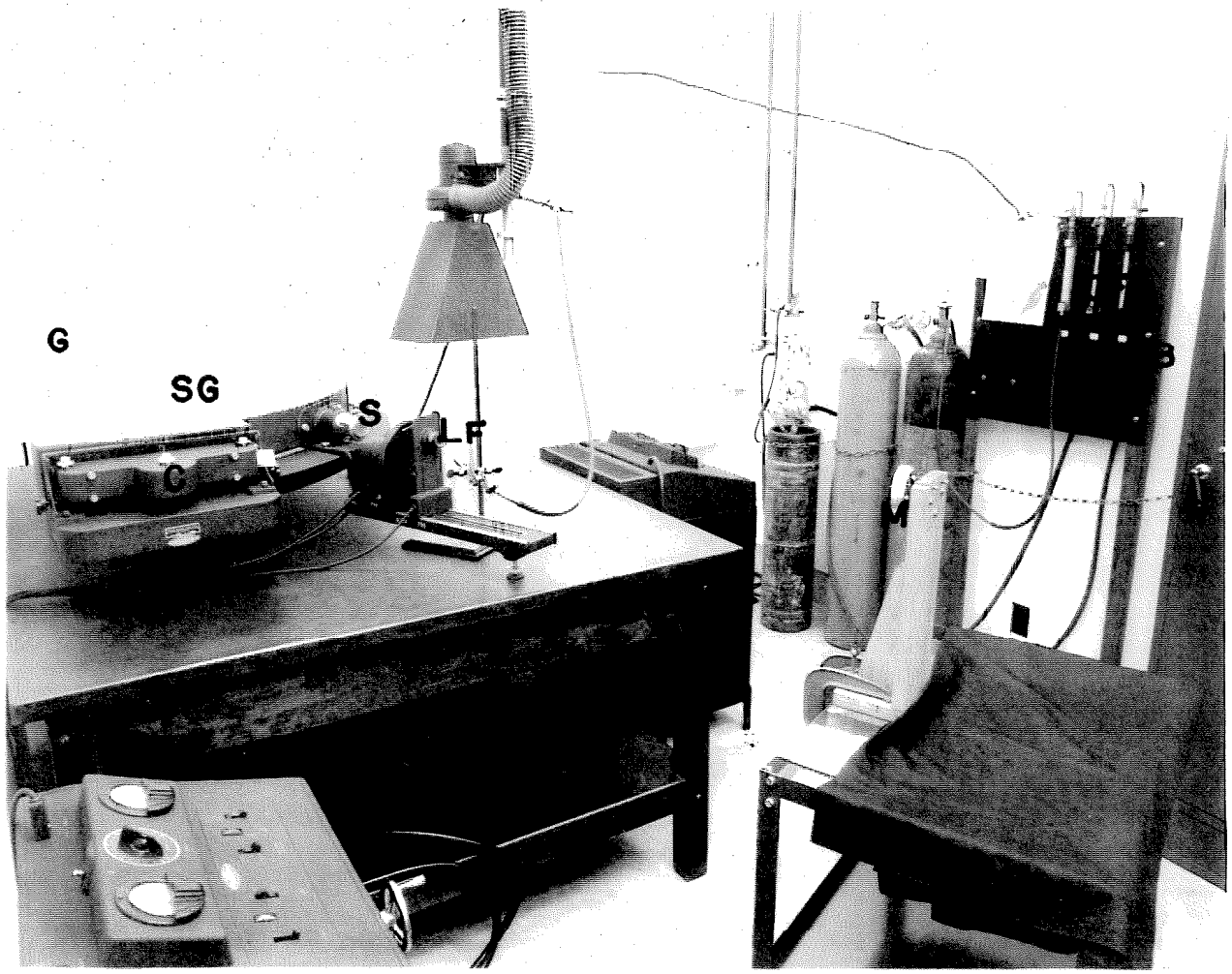

FIG. 12

EXPERIMENTAL APPARATUS

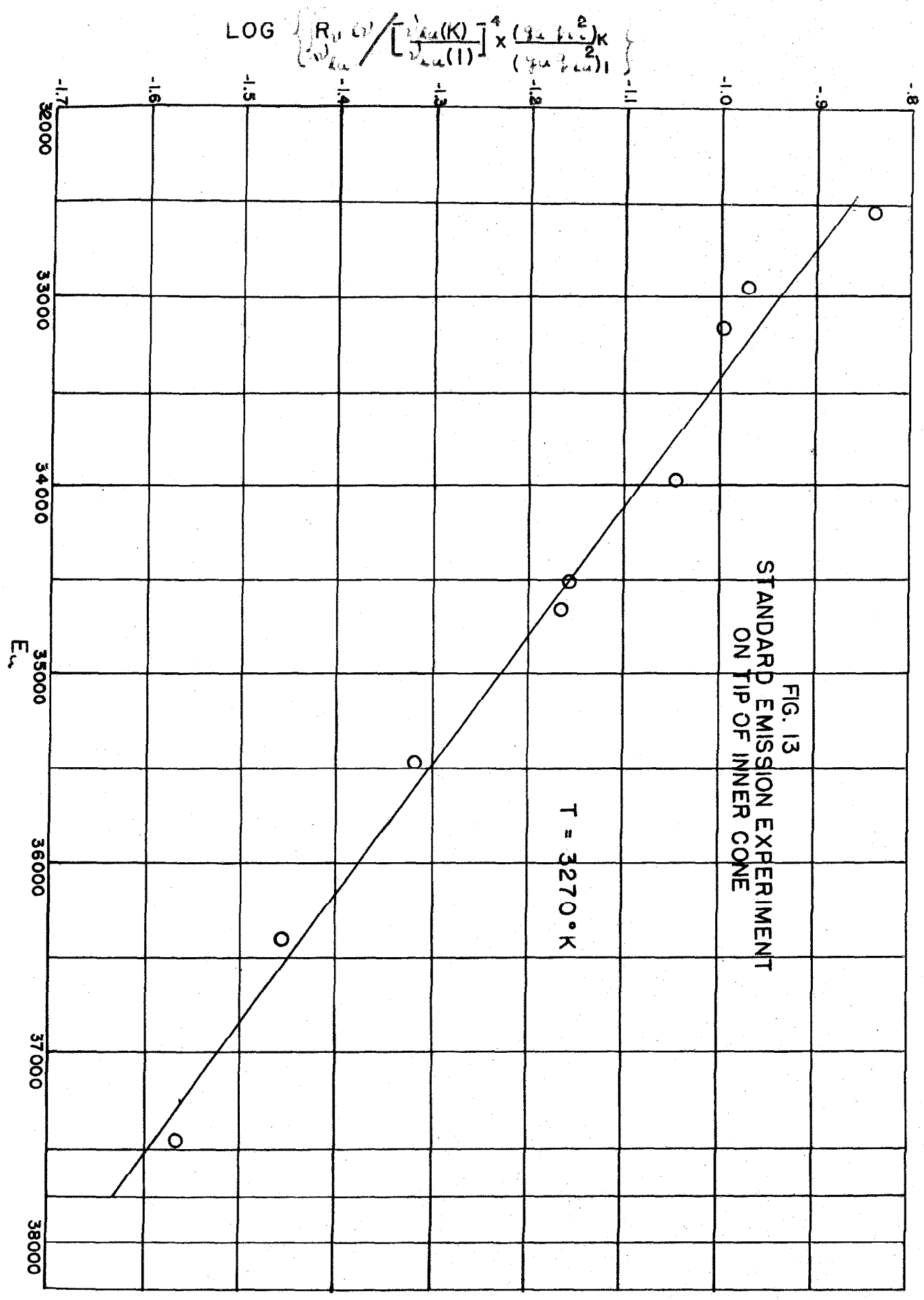

FIG. 13
STANDARD EMISSION EXPERIMENT
ON TIP OF INNER CONE

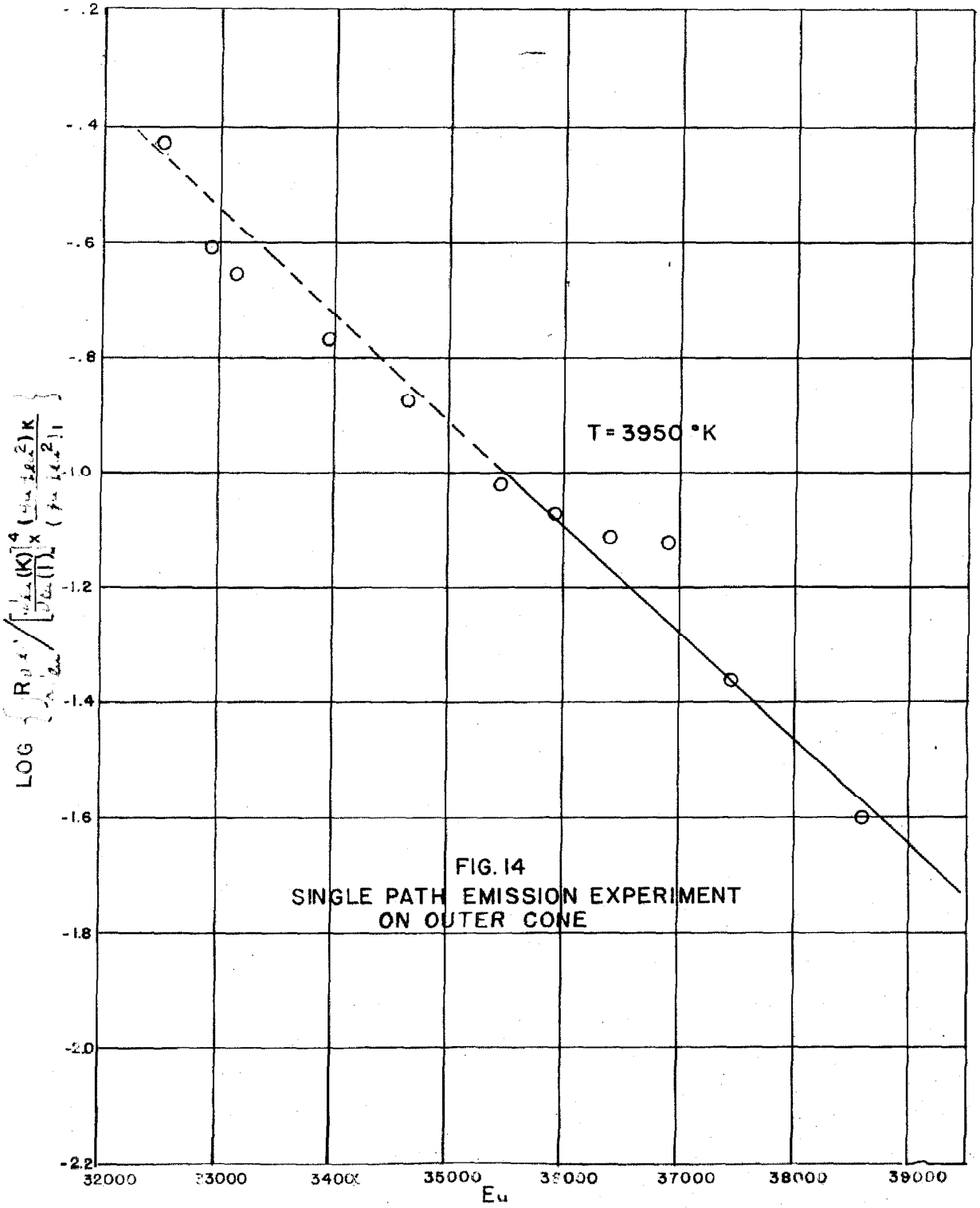

FIG. 14
SINGLE PATH EMISSION EXPERIMENT
ON OUTER CONE

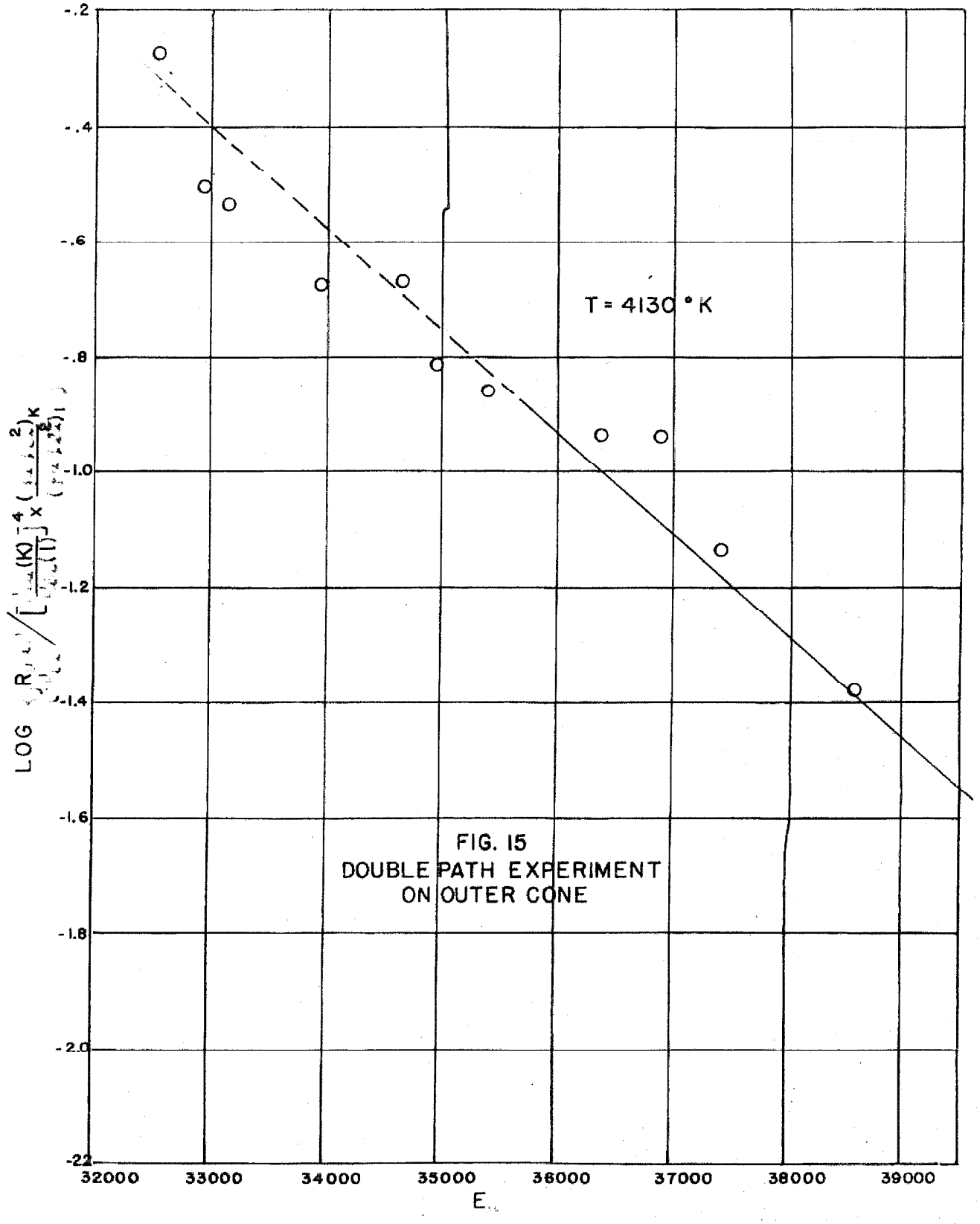

FIG. 15
DOUBLE PATH EXPERIMENT
ON OUTER CONE